

SSNV511 – Block cut out by two interfaces intersected with X-FEM

Summary:

This test makes it possible to validate the approach intersection with X-FEM. It is about a case test where three cracks are introduced. The first crack cuts the field completely. The two other cracks are defined by the same level-set normal. They are connected on both sides of the first via the keyword `JUNCTION` of the operator `DEFI_FISS_XFEM`. The double junction forms an intersection then. One tests the approach with and without contact.

1 Problem of reference

1.1 Geometry

The structure is a healthy square into which one introduces two interfaces, in red on the figure 1.1-a. The two interfaces cross, dimensions of the structure as well as the position of the interfaces are given on this figure.

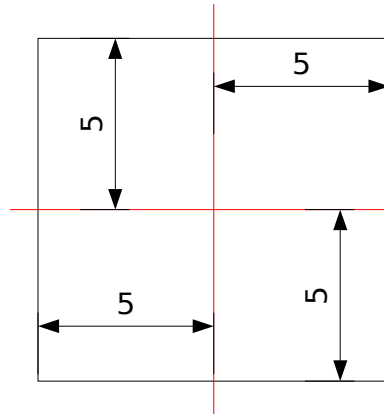


Figure 1.1-a: Geometry of the structure and positioning of the interfaces.

1.2 Properties of material

The material has an isotropic elastic behavior whose properties are:
Young modulus: 100 MPa
Poisson's ratio: 0.3

1.3 Boundary conditions and loadings

In the case without contact (modelings A with D), one applies conditions in displacement to the edges left and right of the structure, so that each of the 4 zones has a displacement different from the others according to X . This loading is represented figure 1.3-a. One blocks displacements in Y (and in Z for modelings 3D) on these same edges. One then obtains displacements of rigid modes for the 4 blocks.

In the case of the contact (modelings E with H), one imposes conditions of roller on the edges left and low and one applies the pressure in staircase of the figure 1.3-b to the flat rims and high. This loading is represented figure 1.3-c. Each block is then compressed in a uniform way according to X and Y .

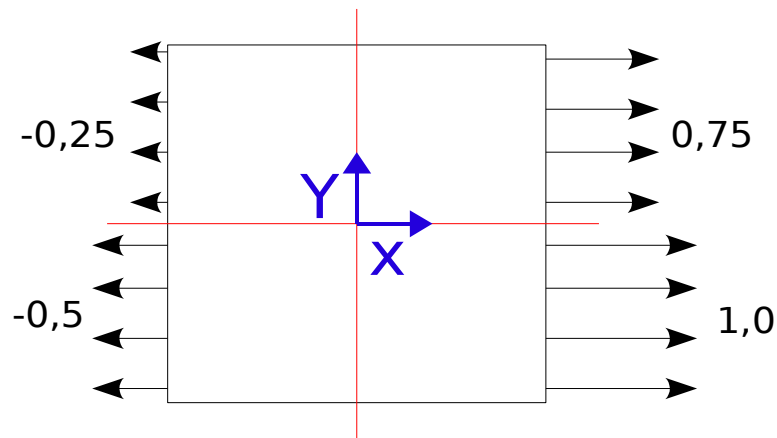


Figure 1.3-a: Illustration of the boundary conditions and the loadings, cases without contact.

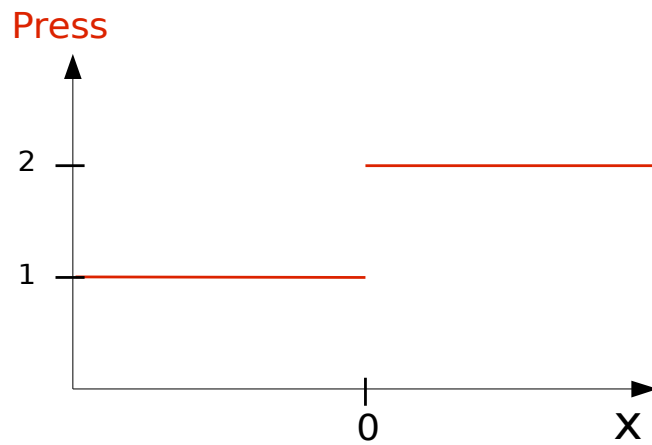


Figure 1.3-b: Pressure imposed according to X on the high edge and according to Y on the flat rim, (in MPa).

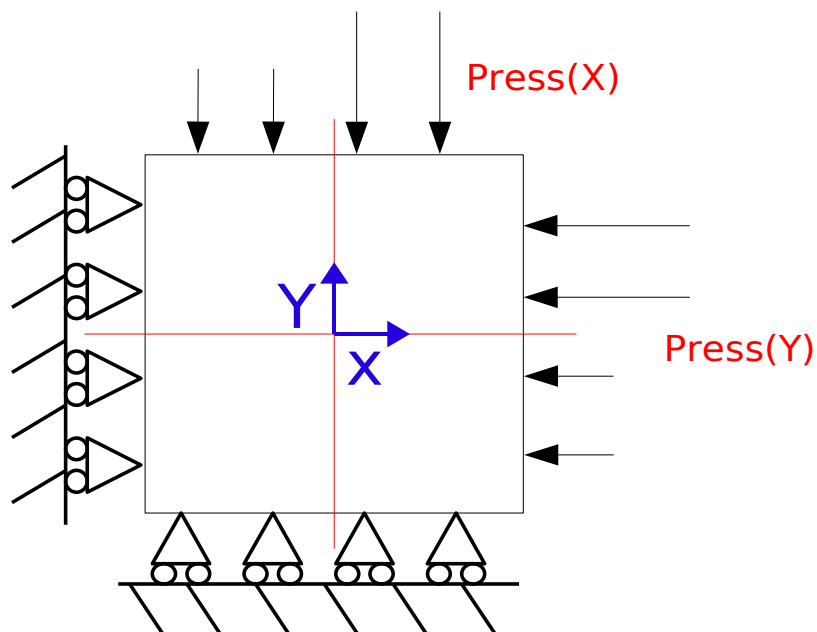


Figure 1.3-c: Illustration of the boundary conditions and the loadings, cases with contact.

2 Reference solution

2.1 Case without contact

Without contact, each zone must undergo a rigid movement of body corresponding to the limiting condition imposed on its edge (right or left).

The energy of the structure is thus:

$$E^e = 0.$$

Shears $\Omega = [-5,5] \times [-5,5]$ the field occupied by the solid. The field of analytical solution displacement is:

$$\mathbf{u} = u_x(x, y) \mathbf{e}_x,$$

with :

$$u_x(x, y) = \begin{cases} -\frac{1}{2} & \text{pour } (x, y) \in [-5, 0[\times [-5, 0[, \\ -1 & \text{pour } (x, y) \in [-5, 0[\times]0, 5], \\ \frac{3}{4} & \text{pour } (x, y) \in]0, 5] \times]0, 5], \\ -\frac{1}{4} & \text{pour } (x, y) \in [-5, 0[\times]0, 5], \end{cases}$$

The standard L^2 displacement is defined by:

$$\|\mathbf{u}\|_{L^2}^2 = \int_{\Omega} \|\mathbf{u}\|^2 dS.$$

One thus has:

$$\|\mathbf{u}\|_{L^2}^2 = 25 \left(\frac{1}{4} + 1 + \frac{9}{16} + \frac{1}{16} \right) = 25 \frac{15}{8}.$$

That is to say:

$$\|\mathbf{u}\|_{L^2} = \frac{5}{2} \sqrt{\frac{15}{2}} \approx 6,84653196881 \text{ m}^2.$$

This result is valid in the case as of plane constraints and of the plane deformations. In the case 3D, the selected thickness is 1 Mr. the expression of the standard L^2 displacement is identical, but the units are modified. One has then:

$$\|\mathbf{u}\|_{L^2} = \frac{5}{2} \sqrt{\frac{15}{2}} \approx 6,84653196881 \text{ m}^{\frac{5}{2}}.$$

2.2 Case with contact

With contact, the 4 blocks undergo a uniform compression according to X and Y . One can express displacement structure in the following way :

$$Depl_X(X, Y) = -(5+X) \frac{Press(Y)}{E} \quad \text{éq 2.1-1}$$

$$Depl_Y(X, Y) = -(5+Y) \frac{Press(X)}{E} \quad \text{éq 2.1-2}$$

3 Modeling A

3.1 Characteristics of modeling

It acts of a modeling X-FEM, into cubesplane formations. The interfaces are defined by functions of levels (level sets noted normals LN).

The equations of the functions of levels for the interfaces horizontal and vertical are the following ones:

$$LN1 = Y \quad \text{éq 3.1-1}$$

$$LN2 = X \quad \text{éq 3.1-2}$$

The horizontal interface is defined in a classical way by using the operator `DEFI_FISS_XFEM` with the level set normal $LN1$.

To define the vertical interface, one proceeds in two stages. The operator for the first time is called `DEFI_FISS_XFEM` with the level set normal $LN2$, by defining a point "in the top" of the horizontal crack for the keyword `JUNCTION` (the point is not obligatorily on the level set). This stage makes it possible to define the upper part of the vertical interface (see figure 3.1-a in the center). The operator for the second time is called `DEFI_FISS_XFEM` same manner, but by defining a point "in lower part" of the crack (see figure 3.1-a on the right).

One thus called on the whole 3 times `DEFI_FISS_XFEM` (creation of 3 cracks objects) to define the two interfaces which are intersected. From a theoretical point of view, each object fissures addition an enrichment of the Heaviside type. What makes a total of three degrees of Heaviside freedom besides the classical degrees of freedom. There are thus well 4 degree of freedom on the level of the intersection, which makes it possible to move in manner independent the 4 zones generated by the 2 interfaces.

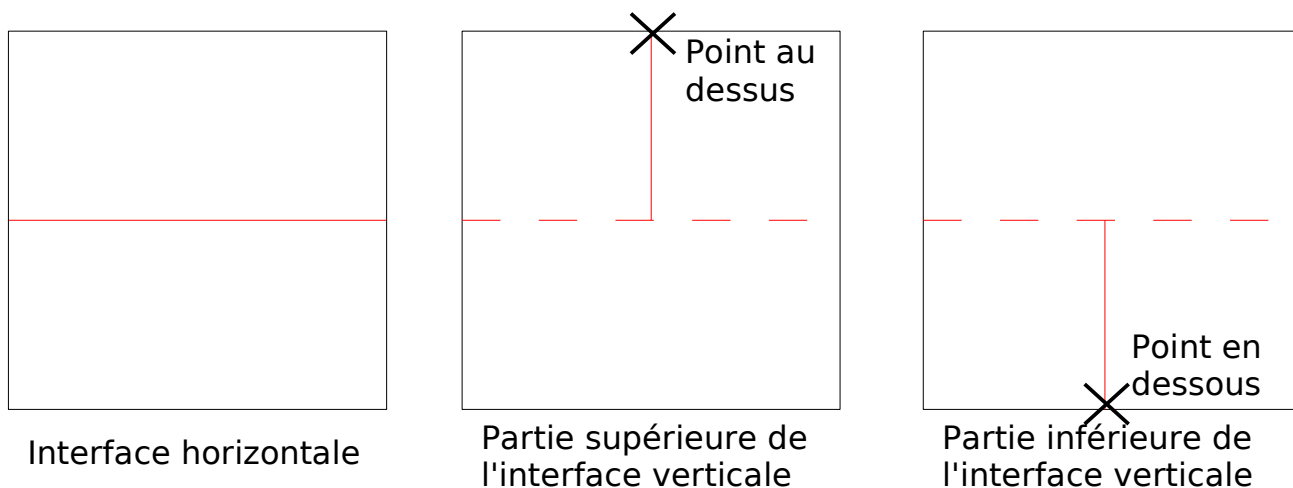


Figure 3.1-a: Stages of construction of the intersection.

3.2 Characteristics of the grid

The grid which comprises 25 meshes of the type `QUAD4`, is represented on the figure 3.2-a.

One notices on this figure that the central mesh is cut by the two interfaces. This test thus makes it possible to validate multiple cutting. Let us note that the nodes of this mesh are nouveau riches 3 times, they thus have the degrees of freedom DX , DY , $H1X$, $H1Y$, $H2X$, $H2Y$, $H3X$ and $H3Y$.

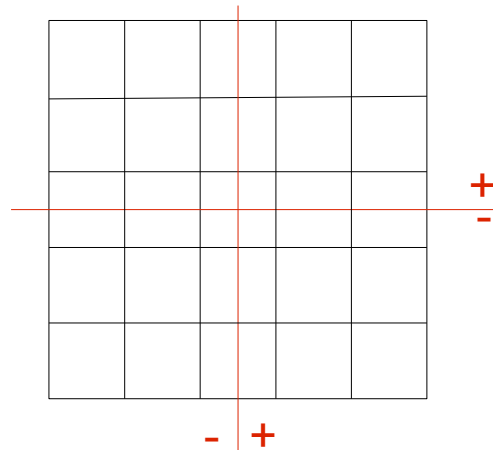


Figure 3.2-a: Grid of modeling A.

3.3 Sizes tested and results

Displacements are tested on the level of the lips of the cracks after having carried out the operations of postprocessings relative to X-FEM (POST_MAIL_XFEM and POST_CHAM_XFEM). Displacement DX must correspond to the loading imposed of the figure 1.3-a on each zone and DY must be null. One tests the min and the max on the lips of each zone.

Identification		Reference	
DEPZON_1	DX	MIN	-0.25
		MAX	-0.25
	DY	MIN	0
		MAX	0
DEPZON_2	DX	MIN	-0.5
		MAX	-0.5
	DY	MIN	0
		MAX	0
DEPZON_3	DX	MIN	0.75
		MAX	0.75
	DY	MIN	0
		MAX	0
DEPZON_4	DX	MIN	0.75
		MAX	0.75
	DY	MIN	0
		MAX	0

Table 3.3-1

The deformation is represented on the figure 3.4-a. The code color represents the field of displacement.

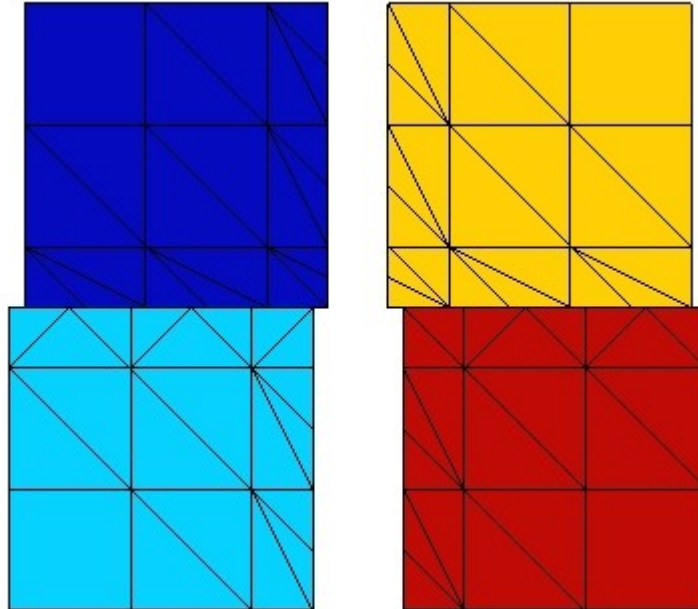


Figure 3.4-a: Deformation of the structure.

One tests the value of E^e product by the operator POST_ERREUR.

Identification	Type of reference	Value of reference
E^e	'ANALYTICAL'	0

One tests the value of $\|u\|_{L^2}$ product by the operator POST_ERREUR.

Identification	Type of reference	Value of reference	Tolerance
L normalizes ²	'ANALYTICAL'	6.84653196881	0.1%

4 Modeling B

4.1 Characteristics of modeling

It is acted of the same modeling as modeling A, but as plane constraints. The intersection is built same manner.

4.2 Characteristics of the grid

The grid which comprises 54 meshes of the type TRIA3 is represented on the figure 4.2-a.

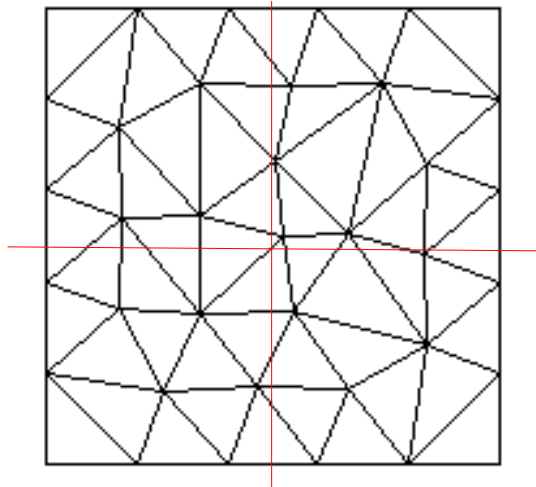


Figure 4.2-a: Grid of modeling B.

4.3 Sizes tested and results

The sizes tested are identical to those presented for modeling A.

Identification		Reference	
DEPZON_1	DX	MIN	-0.25
		MAX	-0.25
	DY	MIN	0
		MAX	0
DEPZON_2	DX	MIN	-0.5
		MAX	-0.5
	DY	MIN	0
		MAX	0
DEPZON_3	DX	MIN	0.75
		MAX	0.75
	DY	MIN	0
		MAX	0
DEPZON_4	DX	MIN	0.75
		MAX	0.75
	DY	MIN	0
		MAX	0

Table 4.3-1

The deformation is represented on the figure 4.4-a.

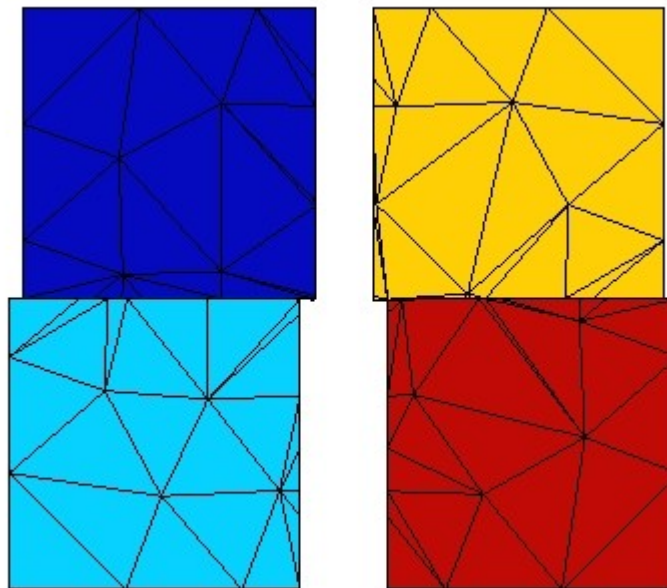


Figure 4.4-a: Deformation of the structure.

One tests the value of E^e product by the operator POST_ERREUR.

Identification	Type of reference	Value of reference
E^e	'ANALYTICAL'	0

One tests the value of $\|u\|_{L^2}$ product by the operator POST_ERREUR.

Identification	Type of reference	Value of reference	Tolerance
L normalizes ²	'ANALYTICAL'	6.84653196881	0.1%

5 Modeling C

5.1 Characteristics of modeling

It is the same modeling as modeling A, but in 3D . The intersection is built same manner.

5.2 Characteristics of the grid

The grid which comprises 25 meshes of the type `HEXA8` is represented on the figure 5.2-a.

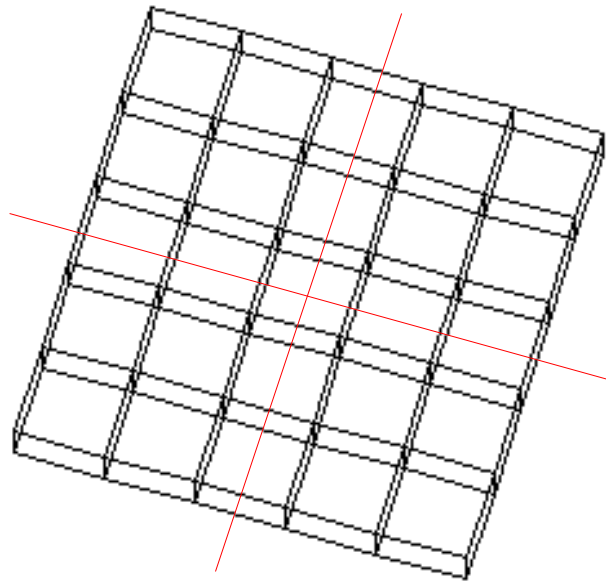


Figure 5.2-a: Grid of modeling C.

5.3 Sizes tested and results

The sizes tested are identical to those presented for modeling A. One adds tests on `DZ`.

Identification		Reference	
DEPZON_1	DX	MIN	-0.25
		MAX	-0.25
	DY	MIN	0
		MAX	0
DEPZON_2	DX	MIN	-0.5
		MAX	-0.5
	DY	MIN	0
		MAX	0
DEPZON_3	DX	MIN	0.75
		MAX	0.75
	DY	MIN	0
		MAX	0
DEPZON_4	DX	MIN	0.75
		MAX	0.75
	DY	MIN	0
		MAX	0

Table 5.3-1

The deformation is represented on the figure 5.4-a.

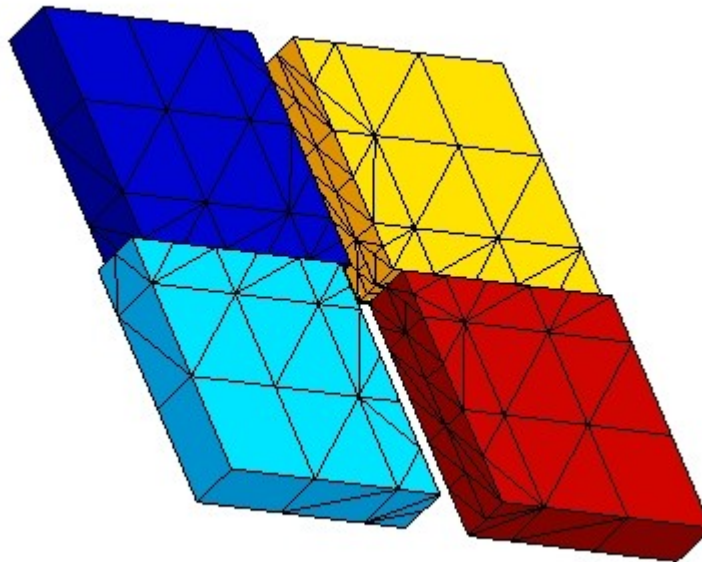


Figure 5.4-a: Deformation of the structure.

One tests the value of E^e product by the operator POST_ERREUR.

Identification	Type of reference	Value of reference
E^e	'ANALYTICAL'	0

One tests the value of $\|u\|_{L^2}$ product by the operator POST_ERREUR.

Identification	Type of reference	Value of reference	Tolerance
L normalizes ²	'ANALYTICAL'	6.84653196881	0.1%

6 Modeling D

6.1 Characteristics of modeling

It is the same modeling as modeling C.

6.2 Characteristics of the grid

The grid which comprises 162 meshes of the type TETRA4 is represented on the figure 6.2-a.

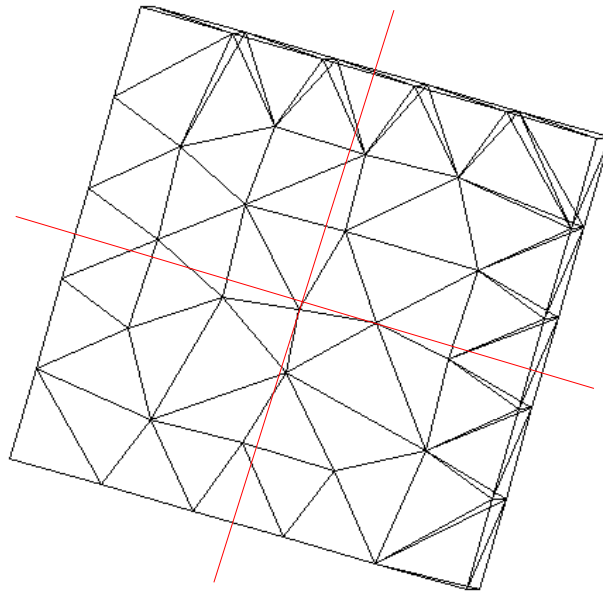


Figure 6.2-a: Grid of modeling D.

6.3 Sizes tested and results

The sizes tested are identical to those presented for modeling C.

Identification		Reference	
DEPZON_1	DX	MIN	-0.25
		MAX	-0.25
	DY	MIN	0
		MAX	0
DEPZON_2	DX	MIN	-0.5
		MAX	-0.5
	DY	MIN	0
		MAX	0
DEPZON_3	DX	MIN	0.75
		MAX	0.75
	DY	MIN	0
		MAX	0
DEPZON_4	DX	MIN	0.75
		MAX	0.75
	DY	MIN	0
		MAX	0

Table 6.3-1

The deformation is represented on the figure 6.4-a.

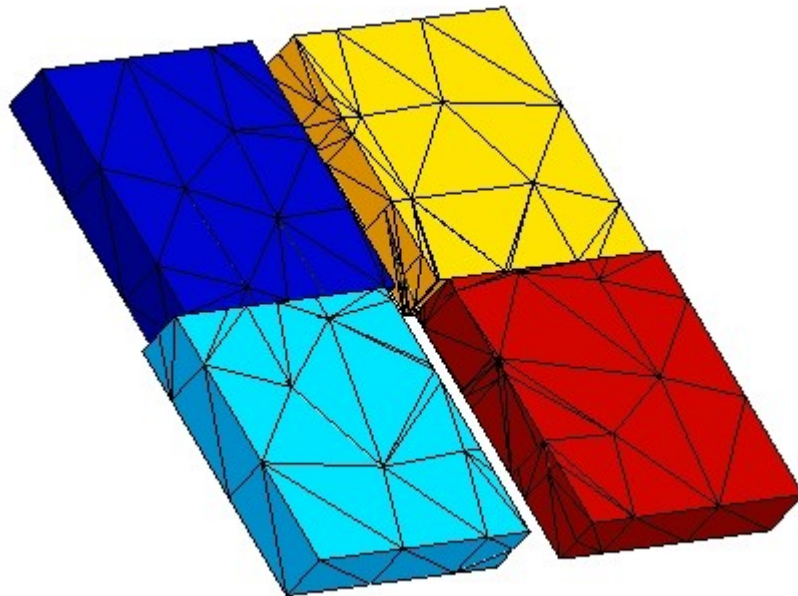


Figure 6.4-a: Deformation of the structure.

7 Modeling E

7.1 Characteristics of modeling

It is the same modeling that modeling A, but the conditions of loading in contact are applied. The intersection is built with X-FEM and the functions of levels in the same way as for modeling A.

7.2 Characteristics of the grid

The grid identical to that of modeling A, is represented figure 3.2-a. Let us note that the nodes of the intersected mesh are nouveau riches 3 times, they thus have the degrees of freedom of contact $LAGS_C$, $LAG2_C$ and $LAG3_C$ besides degrees of freedom kinematics.

7.3 Sizes tested and results

Displacements are tested on the level of the lips of the cracks after having carried out the operations of postprocessings relative to X-FEM ($POST_MAIL_XFEM$ and $POST_CHAM_XFEM$). Displacement D_X must follow the function $Depl_x$ equation 2.1-1. Displacement D_Y must follow the function $Depl_y$ equation 2.1-2. One obtains the deformation of the figure 7.4-a.

Identification		Reference	
DEPZON_1	DX- $Depl_x$	MIN	0
		MAX	0
	DY $Depl_y$	MIN	0
		MAX	0
DEPZON_2	DX- $Depl_x$	MIN	0
		MAX	0
	DY $Depl_y$	MIN	0
		MAX	0
DEPZON_3	DX- $Depl_x$	MIN	0
		MAX	0
	DY $Depl_y$	MIN	0
		MAX	0
DEPZON_4	DX- $Depl_x$	MIN	0
		MAX	0
	DY $Depl_y$	MIN	0
		MAX	0

Table 7.3-1

The deformation is represented on the figure 7.4-a. The code color represents the field of displacement.

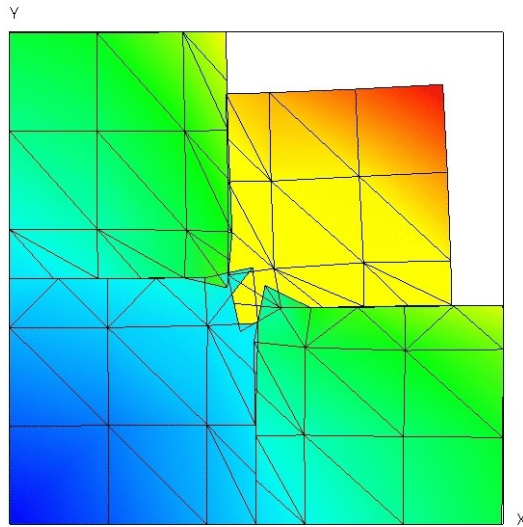


Figure 7.4-a: Deformation of the structure (exaggeration 10).

7.4 Remarks

A high error is obtained. Indeed the implementation of the recutting of the facets of contact was not implemented. The efforts of contact on these facets are not taken into account in calculation. The zone affected relates to in particular the point of intersection of the cracks (which one does not test) as well as the element the container. Let us note that the results are clearly to improve when the grid is refined.

8 Modeling F

8.1 Characteristics of modeling

It is acted of the same modeling as modeling E, but as plane constraints. The intersection is built same manner.

8.2 Characteristics of the grid

The grid identical to that of modeling B, is represented on the figure 4.2-a.

8.3 Sizes tested and results

The sizes tested are identical to those presented for modeling E.

Identification		Reference	
DEPZON_1	DX- $Depl_X$	MIN	0
		MAX	0
	DY $Depl_Y$	MIN	0
		MAX	0
DEPZON_2	DX- $Depl_X$	MIN	0
		MAX	0
	DY $Depl_Y$	MIN	0
		MAX	0
DEPZON_3	DX- $Depl_X$	MIN	0
		MAX	0
	DY $Depl_Y$	MIN	0
		MAX	0
DEPZON_4	DX- $Depl_X$	MIN	0
		MAX	0
	DY $Depl_Y$	MIN	0
		MAX	0

Table 8.3-1

The deformation is represented on the figure 8.4-a.

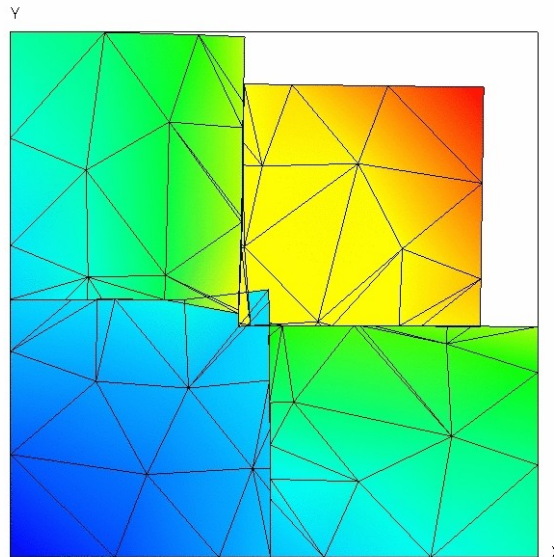


Figure 8.4-a: Deformation of the structure (exaggeration 10).

8.4 Remarks

The remarks are identical to those formulated for modeling E.

9 Modeling G

9.1 Characteristics of modeling

It is the same modeling as modeling E, but in 3D . The intersection is built same manner.

9.2 Characteristics of the grid

The grid identical to that of modeling C, is represented on the figure 5.2-a.

9.3 Sizes tested and results

The sizes tested are identical to those presented for modeling E. One adds tests on DZ .

Identification		Reference	
DEPZON_1	DX- $Depl_x$	MIN	0
		MAX	0
	DY $Depl_y$	MIN	0
		MAX	0
DEPZON_2	DX- $Depl_x$	MIN	0
		MAX	0
	DY $Depl_y$	MIN	0
		MAX	0
DEPZON_3	DX- $Depl_x$	MIN	0
		MAX	0
	DY $Depl_y$	MIN	0
		MAX	0
DEPZON_4	DX- $Depl_x$	MIN	0
		MAX	0
	DY $Depl_y$	MIN	0
		MAX	0

Table 9.3-1

The deformation is represented on the figure 9.4-a.

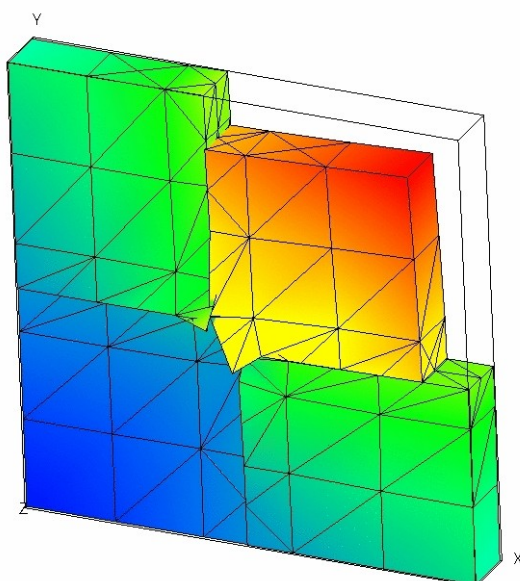


Figure 9.4-a: Deformation of the structure (exaggeration 10).

9.4 Remarks

The remarks are identical to those formulated for modeling E.

10 Modeling H

10.1 Characteristics of modeling

It is the same modeling as modeling G.

10.2 Characteristics of the grid

The grid identical to that of modeling D, is represented on the figure 6.2-a.

10.3 Sizes tested and results

The sizes tested are identical to those presented for modeling G.

Identification		Reference	
DEPZON_1	DX- $Depl_x$	MIN	0
		MAX	0
	DY $Depl_y$	MIN	0
		MAX	0
DEPZON_2	DX- $Depl_x$	MIN	0
		MAX	0
	DY $Depl_y$	MIN	0
		MAX	0
DEPZON_3	DX- $Depl_x$	MIN	0
		MAX	0
	DY $Depl_y$	MIN	0
		MAX	0
DEPZON_4	DX- $Depl_x$	MIN	0
		MAX	0
	DY $Depl_y$	MIN	0
		MAX	0

Table 10.3-1

The deformation is represented on the figure 10.4-a.

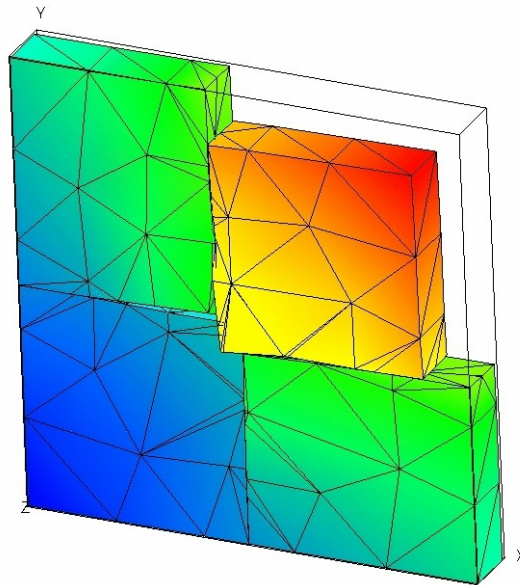


Figure 10.4-a: Deformation of the structure (exaggeration 10).

10.4 Remarks

The remarks are identical to those formulated for modeling E.

11 Summary of the results

The representation of junctions with X-FEM allows to model the kinematics of opening of the intersection of two interfaces. It is also possible to make the same thing with funds of cracks on both sides of the junction, but it is necessary to take care to move away the bottom from the intersection (approximately 2 meshes for a topological enrichment because one cannot manage yet the presence of the additional Heaviside for elements Ace-tip. An element Ace-tip cannot currently “see” more than one crack at the same time).

The approach was validated in 2D for modelings C_PLAN and D_PLAN and for the elements of the type QUAD4 and TRIA3. One also validated the approach in 3D for the elements HEXA8 and TETRA4, with and without contact.